


BRIEF DEFINITIVE REPORT

Nociceptors protect sickle cell disease mice from vaso-occlusive episodes and chronic organ damage

Chunliang Xu^{1,2} , Maria Gulinello³ , and Paul S. Frenette^{1,2,4} 

Sickle cell disease (SCD) is a common hereditary hematologic disorder. SCD patients suffer from acute vaso-occlusive episodes (VOEs), chronic organ damage, and premature death, with few therapeutic options. Although severe pain is a major clinical manifestation of SCD, it remains unknown whether nociception plays a role in SCD pathogenesis. To address this question, we generated nociceptor-deficient SCD mice and found, unexpectedly, that the absence of nociception led to more severe and more lethal VOE, indicating that somatosensory nerves protect SCD mice from VOE. Mechanistically, the beneficial effects of sensory nerves were induced by the neuropeptide calcitonin gene-related peptide (CGRP), which acted on hematopoietic cells. Additionally, oral capsaicin consumption, which can activate somatosensory nerves by binding to TRPV1, dramatically alleviated acute VOE and significantly prevented chronic liver and kidney damage in SCD mice. Thus, the manipulation of nociception may provide a promising approach to treat SCD.

Introduction

Sickle cell disease (SCD), caused by a single missense mutation in the β -globin gene, affects ~100,000 patients in the United States and millions worldwide (Piel et al., 2017; Ware et al., 2017). Mutated β -globin polymerizes under deoxygenation, leading to sickle-shaped RBCs, which exhibit increased adherence to other blood cells or to the endothelium and are prone to undergo premature clearance and hemolysis (Sundd et al., 2019). The RBC alterations lead to a chronic inflammatory state, resulting in ischemic tissue damage, manifested by severe pain and organ failure. Acute vaso-occlusive episodes (VOEs) and chronic organ damage are the hallmarks of SCD, although it is not clear how the latter is related to the former. The pathophysiology of VOE and chronic organ damage is complex and involves the interplay of altered blood rheology, endothelial activation, and the secretion of inflammatory cytokines enabling leukocyte adhesion and activation (Zhang et al., 2016). Intravital microscopy analysis of the SCD mouse microcirculation has revealed that RBCs interact with adherent leukocytes in the inflamed vasculature (Turhan et al., 2002). The accumulation of activated neutrophils interacting with RBCs progressively reduces blood flow and produces venular occlusions (Chiang et al., 2007; Hidalgo et al., 2009). Further studies suggest that the aged neutrophil subset (marked by low CD62L and high CXCR4 expression; Casanova-Acebes et al., 2013; Van Eeden et al., 1997) is

the most active leukocyte subset driving VOE and possibly contributing to chronic organ damage in a humanized SCD mice model (Zhang et al., 2015).

Pain is the most frequent reason for hospital visits among SCD patients (Aich et al., 2019; Ballas et al., 2012; Piel et al., 2017; Ware et al., 2017). While acute and chronic pain may coexist in SCD patients, their mechanisms may partially overlap (Aich et al., 2019; Ballas et al., 2012). Recent studies using a humanized SCD mouse model have revealed that hyperalgesia in SCD was caused by substance P, prostaglandin E₂, and chemokine receptor 2 (Aich et al., 2019; Khasabova et al., 2019; Sadler et al., 2018; Vincent et al., 2013). The pain in SCD (and other conditions) is largely sensed by the transient receptor potential vanilloid 1 (TRPV1; Hillery et al., 2011), which confers sensitivity to heat (Basbaum et al., 2009) and is activated by its natural ligand, capsaicin (Caterina et al., 1997).

Nociceptive nerves are present in every tissue in the body and are excited when thermal, mechanical, or chemical stimuli reach the noxious range. The sensory nervous system has recently emerged as a critical regulator of the immune response (Baral et al., 2018; Chiu et al., 2013; Cohen et al., 2019; Godinho-Silva et al., 2019; Nagashima et al., 2019; Oetjen et al., 2017; Riolo-Blanco et al., 2014; Talbot et al., 2015). In particular, sensory nerves were reported to regulate neutrophils, group 2 innate

¹The Ruth L. and David S. Gottesman Institute for Stem Cell and Regenerative Medicine Research, Albert Einstein College of Medicine, Bronx, NY; ²Department of Cell Biology, Albert Einstein College of Medicine, Bronx, NY; ³Dominick P. Purpura Department of Neuroscience, Albert Einstein College of Medicine, Bronx, NY; ⁴Department of Medicine, Albert Einstein College of Medicine, Bronx, NY.

Correspondence to Paul S. Frenette: paul.frenette@einsteinmed.org.

© 2020 Xu et al. This article is distributed under the terms of an Attribution–Noncommercial–Share Alike–No Mirror Sites license for the first six months after the publication date (see <http://www.rupress.org/terms/>). After six months it is available under a Creative Commons License (Attribution–Noncommercial–Share Alike 4.0 International license, as described at <https://creativecommons.org/licenses/by-nc-sa/4.0/>).

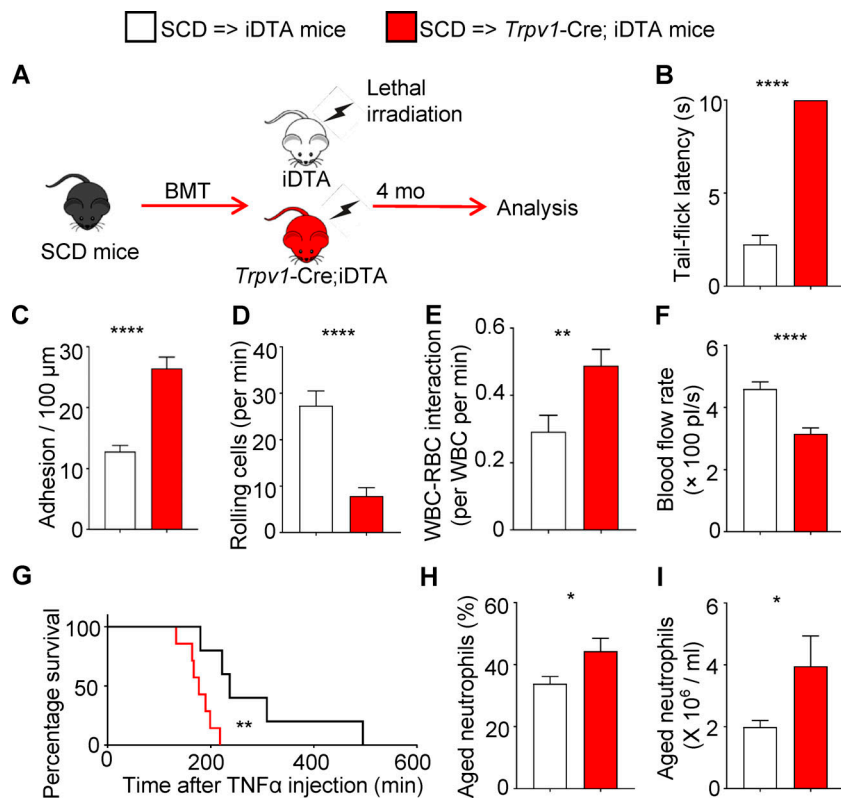


Figure 1. Depletion of nociceptors predisposes SCD mice to VOE. (A) Diagram of experimental design. (B) Tail flick assay 4 mo after transplantation confirming the absence of hot sensation in the SCD \rightarrow *Trpv1-Cre*; iDTA mice ($n = 4$ /group). (C–F) Number of adherent leukocytes (C), rolling leukocytes (D), and WBC-RBC heterotypic interactions (E) and blood flow rate (F) in the postcapillary collecting venules of cremaster muscle in SCD \rightarrow iDTA mice ($n = 34$ venules from five mice) and SCD \rightarrow *Trpv1-Cre*; iDTA mice ($n = 35$ from seven mice) analyzed by intravital microscopy. (G) Survival time of SCD \rightarrow iDTA mice ($n = 5$) and SCD \rightarrow *Trpv1-Cre*; iDTA mice ($n = 7$) in TNF α -induced acute vaso-occlusion. (H and I) Percentage of aged neutrophils (H) and absolute number of aged neutrophils (I) in peripheral blood of SCD \rightarrow iDTA mice ($n = 8$) and SCD \rightarrow *Trpv1-Cre*; iDTA mice ($n = 4$) mice. Error bars, mean \pm SEM; *, $P < 0.05$; **, $P < 0.01$; ***, $P < 0.001$; ****, $P < 0.0001$. Data represent at least two independent experiments analyzed using unpaired Student's *t* test in B–F, H, and I and Mantel–Cox test (log-rank) for the survival analysis in G.

lymphoid cells, and T cells via calcitonin gene-related peptide (CGRP) released from nerve terminals in both skin and lung (Baral et al., 2018; Cohen et al., 2019; Nagashima et al., 2019; Pinho-Ribeiro et al., 2018; Wallrapp et al., 2019). Because pain sensation is the major clinical manifestation of SCD, we asked whether, and if so how, pain affects the inflammatory response that plays a key role in SCD.

Results and discussion

Depletion of nociceptors predisposes SCD mice to VOE

To study the effect of pain in SCD, we bred *Trpv1-Cre* mice with transgenic mice in which the diphtheria toxin fragment A can be conditionally expressed (iDTA) to obtain *Trpv1-Cre*; iDTA animals, leading to the elimination of TRPV1-expressing nociceptors. To generate nociceptor-deficient and control SCD mice, we transplanted bone marrow nucleated cells from Berkeley SCD mice into lethally irradiated *Trpv1-Cre*; iDTA (SCD \rightarrow *Trpv1-Cre*; iDTA) and iDTA control (SCD \rightarrow iDTA) animals (Fig. 1 A). Donor SCD engraftment in the bone marrow of *Trpv1-Cre*; iDTA and iDTA recipients was similar (>97%; not depicted). To confirm the efficiency of the deletion, we subjected recipient mice to a tail flick assay in hot water and found that control SCD \rightarrow iDTA mice lifted their tails within 3 s, whereas the SCD \rightarrow *Trpv1-Cre*; iDTA animals kept their tails in the hot water for >10 s (10 s was used as cutoff to avoid excessive damage; Fig. 1 B). These results indicate that nociceptors were efficiently depleted in SCD \rightarrow *Trpv1-Cre*; iDTA mice.

To determine the role of somatosensory nerves in VOE, we compared the VOE responses between SCD \rightarrow *Trpv1-Cre*; iDTA

mice and SCD \rightarrow iDTA controls using the TNF α -induced VOE model (Turhan et al., 2002; Zhang et al., 2015). Surprisingly, we observed an exaggerated inflammatory response in SCD \rightarrow *Trpv1-Cre*; iDTA mice, manifested by significant elevations of leukocyte adhesion, reduced rolling fraction, and increased rate of interactions between RBC and leukocytes by intravital microscopy (Fig. 1, C–E). In addition, the mean centerline RBC velocities, blood flow rate, and wall shear rate were all significantly reduced in SCD \rightarrow *Trpv1-Cre*; iDTA mice compared with SCD \rightarrow iDTA control animals, suggesting a more severe vaso-occlusion in nociceptor-depleted animals (Fig. 1 F and Table S1). SCD \rightarrow *Trpv1-Cre*; iDTA mice also succumbed to the acute vaso-occlusive challenge significantly faster than SCD \rightarrow iDTA animals (median survival time, 237 and 177 min, respectively; Fig. 1 G). Although we found no significant difference in the severity of anemia between SCD \rightarrow *Trpv1-Cre*; iDTA and SCD \rightarrow iDTA mice (Fig. S1, A–C), the number of circulating aged neutrophils, which were previously suggested to drive VOE in humanized SCD mice (Zhang et al., 2015), was significantly elevated in the SCD \rightarrow *Trpv1-Cre*; iDTA mice (Fig. 1, H and I). These data suggest that the nociceptive pathway protects SCD mice from VOE.

CGRP mediates the protective effects of nociceptive pathway

CGRP, released from activated sensory nerve terminals, is a potent vasodilator that has also been suggested to regulate inflammation (Baral et al., 2018; Nagashima et al., 2019; Wallrapp et al., 2019). To investigate whether this neurotransmitter mediated the protective effect of sensory nerve, we administered CGRP or vehicle using a slow-releasing micropump and analyzed

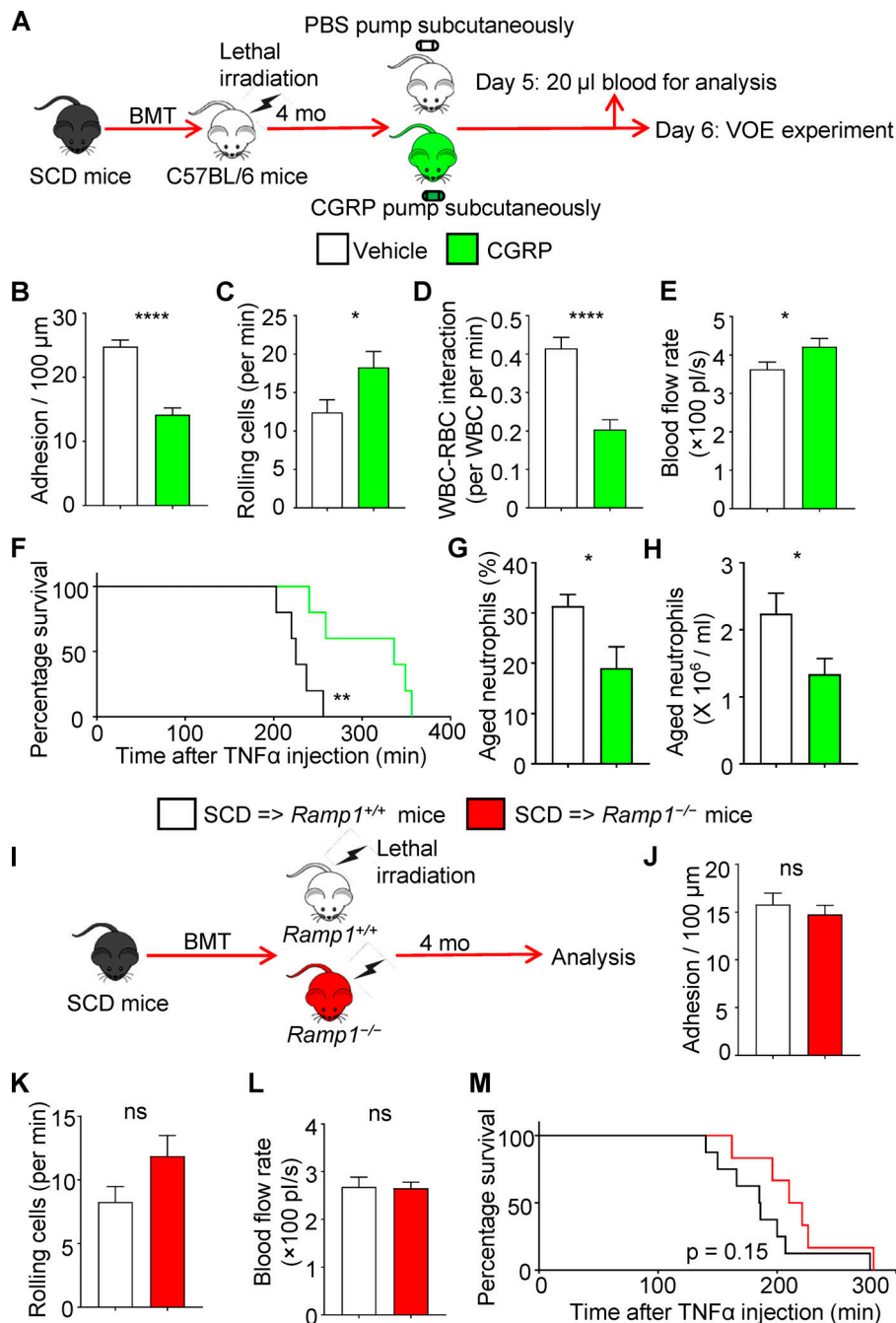


Figure 2. CGRP mediates the protective effects of nociceptive pathway. (A) Diagram of experimental design. (B–E) Number of adherent leukocytes (B), rolling leukocytes (C), and WBC-RBC heterotypic interactions (D) and blood flow rate (E) in the postcapillary collecting venules of cremaster muscle in vehicle-treated SCD mice ($n = 52$ venules from five mice) and CGRP-treated SCD mice ($n = 43$ venules from five mice) analyzed by intravital microscopy. (F) Survival time of vehicle-treated SCD mice ($n = 5$) and CGRP-treated SCD mice ($n = 5$) in TNF α -induced acute vaso-occlusion. (G and H) Percentage of aged neutrophils (G) and absolute number of aged neutrophils (H) in peripheral blood of vehicle-treated SCD mice ($n = 5$) and CGRP-treated SCD mice ($n = 5$). (I) Diagram of experimental design. (J–L) Number of adherent leukocytes (J) and rolling leukocytes (K) and blood flow rate (L) in the postcapillary collecting venules of cremaster muscle in SCD \rightarrow *Ramp1*^{+/+} mice ($n = 30$ venules from eight mice) and SCD \rightarrow *Ramp1*^{-/-} mice ($n = 37$ venules from six mice) analyzed by intravital microscopy. (M) Survival time of SCD \rightarrow *Ramp1*^{+/+} mice ($n = 8$ mice) and SCD \rightarrow *Ramp1*^{-/-} mice ($n = 6$ mice) in TNF α -induced acute vaso-occlusion. Error bars, mean \pm SEM; *, $P < 0.05$; **, $P < 0.01$; ***, $P < 0.001$; ****, $P < 0.0001$. Data represent at least two independent experiments analyzed using unpaired Student's t test in B–E, G, H, and J–L and Mantel–Cox test (log-rank) for the survival analysis in F and M. ns, not significant.

these mice 6 d after the initiation of treatment (Fig. 2 A). Interestingly, the inflammatory response was reduced in CGRP-treated SCD mice, as evidenced by significant reduction in leukocyte adhesion, increased rolling fraction, and reduced rates of interactions between RBC and leukocytes (Fig. 2, B–D), suggesting that CGRP inhibited leukocyte activation. In addition, the mean centerline RBC velocities, blood flow rate, and wall shear rate were all significantly improved in CGRP-treated SCD mice compared with vehicle-treated SCD mice (Fig. 2 E and Table S2). Moreover, the survival time of CGRP-treated SCD mice was greatly prolonged compared with control mice (Fig. 2 F), suggesting that CGRP released from activated somatosensory nerves mediated the protective effect of nociceptors

against VOE. Hematologic analysis showed no difference in the degree of anemia between vehicle-treated and CGRP-treated SCD mice (Fig. S1, D and E). FACS analysis of the peripheral blood cells revealed significant reductions of aged neutrophil numbers in CGRP-treated SCD mice (Fig. 2, G and H). As activation of the CGRP receptor results in G_{α_s} -mediated activation of adenylate cyclase (AC), causing accumulation of cAMP (Russell et al., 2014), we tested whether stimulation of AC with forskolin, an AC activator, could mimic the effect of CGRP in protecting SCD mice from VOE. Interestingly, forskolin, like CGRP, protected SCD mice from VOE, as shown by the reduced inflammatory response (Fig. S2, A and B), significant improvement of blood flow (Fig. S2 C and Table S3), and prolonged

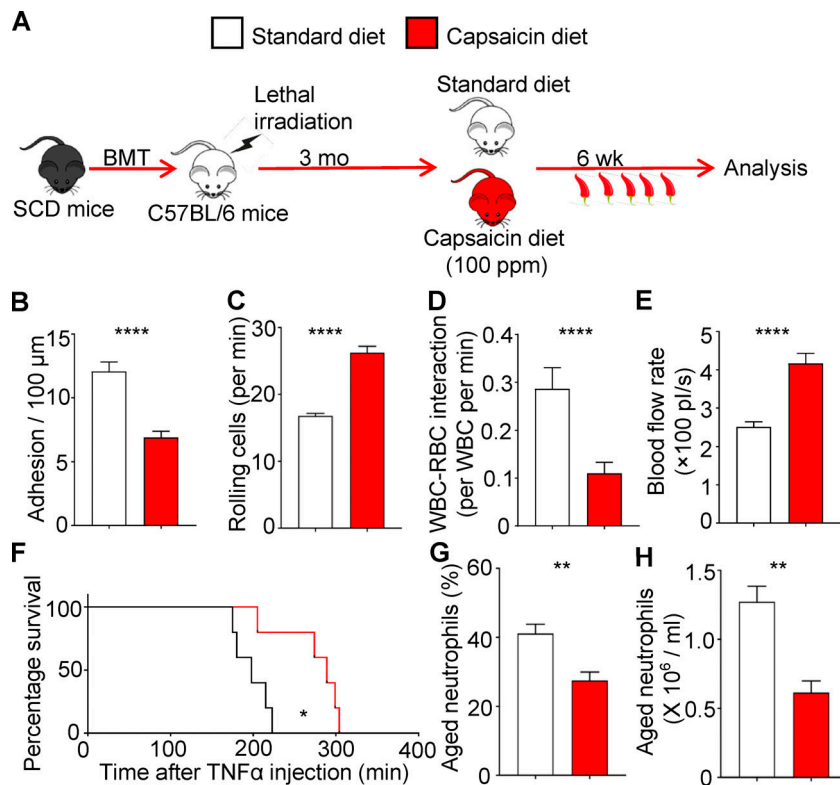


Figure 3. Short-term capsaicin diet protects SCD mice from VOE. (A) Diagram of experimental design. (B–E) Number of adherent leukocytes (B), rolling leukocytes (C), and WBC–RBC heterotypic interactions (D) and blood flow rate (E) in the postcapillary collecting venules of cremaster muscle in standard diet-treated SCD mice ($n = 41$ venules from five mice) and capsaicin diet-treated SCD mice ($n = 47$ venules from five mice) analyzed by intravital microscopy. (F) Survival time of standard diet-treated SCD mice ($n = 5$) or capsaicin diet-treated SCD mice ($n = 5$) in TNF α -induced acute vaso-occlusion. (G and H) Percentage of aged neutrophils (G) and absolute number of aged neutrophils (H) in peripheral blood of standard diet-treated SCD mice ($n = 5$) or capsaicin diet-treated SCD mice ($n = 5$). Error bars, mean \pm SEM; *, $P < 0.05$; **, $P < 0.01$; ***, $P < 0.001$; ****, $P < 0.0001$. Data represent at least two independent experiments analyzed using unpaired Student's t test in B–E, G, and H and Mantel–Cox test (log-rank) for the survival analysis in F.

survival time (Fig. S2 D). Nociceptors thus inhibit VOE through CGRP.

To get more mechanistic insights into how CGRP protects the SCD mice from VOE, we generated SCD mice in which non-hematopoietic cells are deficient in CGRP receptors. Receptor activity-modifying protein 1 (RAMP1), together with calcitonin receptor-like receptor (CALCRL), form the CGRP receptor and mediate its downstream signaling (McLatchie et al., 1998). We transplanted bone marrow cells from SCD mice into lethally irradiated *Ramp1*^{+/+} and *Ramp1*^{-/-} mice to generate SCD \rightarrow *Ramp1*^{+/+} and SCD \rightarrow *Ramp1*^{-/-} animals, respectively (Fig. 2I). We then challenged these mice with VOE and found that *Ramp1* deletion in nonhematopoietic cells had no effect on the outcome of VOE (Fig. 2, I–M; and Table S4), suggesting that CGRP exerts its protective effects by acting on hematopoietic cells. Neutrophils, especially aged neutrophils, drive VOE in SCD mice (Chiang et al., 2007; Hidalgo et al., 2009; Turhan et al., 2002; Zhang et al., 2016). Our results suggest that CGRP reduces aged neutrophil numbers and activity (Fig. 2, G and H), which is consistent with recent studies in the context of a *Streptococcus pyogenes* infection (Pinho-Ribeiro et al., 2018). Taken together, these results support a model in which the activation of nociceptors in SCD mice leads to the release of CGRP, which inhibits aged neutrophil accumulation and subsequent VOE.

Short-term capsaicin diet protects SCD mice from VOE

As the chili pepper extract capsaicin is a natural ligand of TRPV1 (Caterina et al., 1997), we hypothesized that low-grade activation of nociceptors resulting from spicy food ingestion might mitigate VOE severity in SCD mice. To test this idea, we fed SCD mice for 6 wk with a diet containing capsaicin (100 ppm) and

analyzed their response to VOE challenge (Fig. 3 A). The capsaicin-containing diet had no effects on the consumption of food or water (Fig. S3, A and B), body weight (Fig. S3 C), or the degree of anemia of SCD mice (Fig. S3, D and E). Intravital microscopy analyses revealed that the addition of capsaicin in the diet significantly reduced the number of adherent white blood cells (WBCs) and WBC–RBC heterotypic interactions while significantly increasing the number of rolling leukocytes compared with standard diet (Fig. 3, B–D). In addition, the mean centerline RBC velocities, blood flow rate, and wall shear rate were all significantly improved in SCD mice that consumed spicy food compared with controls, suggesting that capsaicin can mitigate acute vaso-occlusion (Fig. 3 E and Table S5). We also found that the survival time after the VOE challenge was significantly prolonged in mice fed with capsaicin-containing diet compared with standard chow (Fig. 3 F). Interestingly, the capsaicin diet, like CGRP, significantly reduced the number of aged neutrophils in the circulation (Fig. 3, G and H). These results suggest that a diet containing a TRPV1 agonist dramatically mitigates vaso-occlusive events.

Long-term capsaicin diet protects SCD mice from chronic organ damage

Chronic organ damage is another major hallmark of SCD and the key cause of mortality. Although chronic organ damage might result from repeated cycles of VOE and ischemia-reperfusion injury (Nath and Hebbel, 2015), whether it is the case is not certain. For example, SCD mice lacking the integrin $\alpha_M\beta_2$ are protected from acute VOE, but no impact on organ damage was observed (Chen et al., 2016). Given the improved response to VOE challenge by dietary spicy food, we tested whether chronic

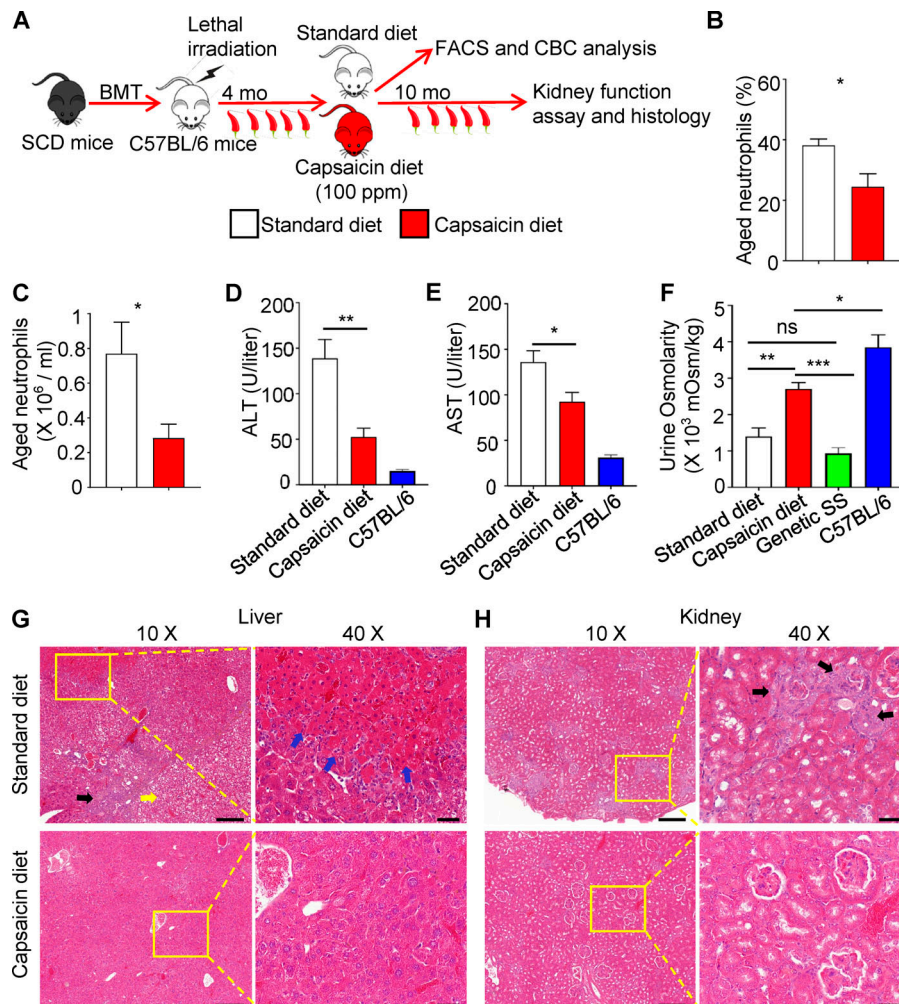


Figure 4. Long-term capsaicin diet protects SCD mice from chronic organ damage. (A) Diagram of experimental design. CBC, complete blood count. (B and C) Percentage of aged neutrophils (B) and absolute number of aged neutrophils (C) in peripheral blood of standard diet-treated SCD mice ($n = 5$) or capsaicin diet-treated SCD mice ($n = 5$) 4 mo after treatment. (D and E) Plasma ALT (D) and AST (E) concentrations in standard diet-treated SCD mice ($n = 5$), capsaicin diet-treated SCD mice ($n = 5$) 4 mo after treatment, and wild-type C57BL/6 mice ($n = 5$). (F) Quantification of urine osmolality of standard diet-treated SCD mice ($n = 4$), capsaicin diet-treated SCD mice ($n = 4$) 14 mo after treatment, genetic SCD mice ($n = 6$), and wild-type C57BL/6 mice ($n = 4$). (G) Representative H&E staining of livers from SCD mice fed with standard or capsaicin diet. Note the hemorrhagic necrotic area (blue arrows), steatosis/necrosis (yellow arrow), and leukocyte infiltration (black arrow) in liver sample from a SCD mouse fed with standard chow. Scale bars = 100 μ m; 20 μ m (inset). (H) Representative H&E staining of kidneys from SCD mice fed with standard chow or capsaicin-containing chow. Note the accumulation of inflammatory cells around glomeruli (glomerulonephritis) in the kidney from SCD mice fed with standard chow (black arrows). Scale bars = 200 μ m; 40 μ m (inset). Error bars, mean \pm SEM; *, $P < 0.05$; **, $P < 0.01$; ***, $P < 0.001$; ****, $P < 0.0001$. Data represent at least two independent experiments analyzed using unpaired Student's *t* test in B–E or one-way ANOVA using Tukey's multiple comparisons test in F. ns, not significant.

capsaicin consumption could mitigate liver and kidney damage (Fig. 4 A). We found that a long-term (4-mo) capsaicin diet also reduced the number of circulating aged neutrophils (Fig. 4, B and C). Strikingly, the liver injury, as measured by elevated aspartate transaminase (AST) and alanine transaminase (ALT) enzyme levels in plasma, was significantly improved in SCD mice fed for 4 mo on capsaicin-containing chow compared with standard chow (Fig. 4, D and E). Kidney failure is among the most devastating events in SCD patients (Nath and Hebbel, 2015). Compared with SCD mice born with the disease, SCD animals generated by bone marrow transplantation (BMT) develop damage to the kidney at a later stage than to the liver (Nasimuzzaman et al., 2019). Accordingly, we continued the treatment for 14 mo to evaluate the impact on kidney function and anemia. We did not observe any change in the degree of anemia (Fig. S3, F and G) or obvious behavioral abnormalities after long-term treatment of SCD mice (Video 1 and Video 2). Analysis of kidney function by measuring urine osmolality after overnight water deprivation revealed that BMT SCD mice developed significant kidney damage 14 mo after BMT, to a level similar to that of age-matched parental SCD mice (Fig. 4 F). Interestingly, the capsaicin diet markedly improved kidney function in BMT SCD mice (Fig. 4 F). We confirmed the beneficial effect by histological analysis of kidneys and livers from

standard or capsaicin diet-treated SCD mice (Fig. 4, G and H). Capsaicin is used topically to treat pain from a wide range of chronic conditions (Derry et al., 2009). To test whether long-term consumption of a capsaicin diet altered pain perception, we analyzed the sensitivity of SCD mice to a heat stimulus using the Hargreaves test (Hargreaves et al., 1988). Our results showed that the capsaicin diet did not change the response of SCD mice to a noxious heat stimulus, as shown by similar paw withdrawal latency between standard or capsaicin diet-treated SCD mice (Fig. S3 H). These data thus demonstrate the protective effects of capsaicin diet in the development of liver and kidney damage in humanized SCD mice, possibly through CGRP release, suggesting that manipulation of the nociceptive pathway by diet is a promising method to preserve target organs without affecting nociception.

Concluding remarks

Under normal circumstances, pain is an evolutionarily conserved protective mechanism to alarm the host and avoid noxious stimuli. Excessive pain, however, can be detrimental to human health and a source of disease manifestation in SCD. Although much effort has been dedicated to alleviate pain in SCD, our results indicate, surprisingly, that depletion of nociceptors exacerbates VOE, and that, conversely, the activation of

nociceptors using a capsaicin-containing diet protects humanized SCD mice from both VOE and organ damage. These data echo the evolutionarily conserved benefit of pain pathways and argue that current pain management methods, counterintuitively, may predispose SCD patients to VOE and organ damage. This hypothesis is in line with observations suggesting that SCD patients on chronic opioid treatment may have poorer functional outcomes and more hospitalization than the control cohort (Carroll et al., 2016). Mechanistically, our results suggest that it is not the pain perception, but rather CGRP release, that mediates the protective effect of nociceptors. Thus, drugs reducing pain perception without affecting CGRP release would be most suitable for pain management. CGRP administration or induction of cAMP by forskolin treatment, or a diet containing the TRPV1 ligand capsaicin, all reduced excessive inflammation during tissue injury. Our results point to an inherent protective mechanism of nociceptors, and shed new light on potential novel disease-modifying targets to treat SCD.

Materials and methods

Mice

Tg[Hu-miniLCR α 1^{C γ} δ β ^S] *Hba*^{-/-} *Hbb*^{-/-} mice (Berkeley sickle cell mice) are bred in the laboratory and have been used in previous studies (Hidalgo et al., 2009; Turhan et al., 2002; Zhang et al., 2015). B6.129-Trpv1tm1(cre)Bbm/J (*Trpv1*-Cre) and B6.129P2-Gt(ROSA)26Sortm1(DTA)Lky/J (*iDTA*) mice were purchased from the Jackson Laboratory. *Ramp1*^{-/-} mice were a gift from Dr. Kathleen M. Caron (University of North Carolina, Chapel Hill, NC; Li et al., 2014), and littermate controls were used in our experiments. C57BL/6 mice were purchased from Charles River Laboratories. All mice were housed in specific pathogen-free conditions and fed with autoclaved food. Experimental procedures were approved by the Animal Care and Use Committee of Albert Einstein College of Medicine.

BMT

SCD mouse cohorts were generated by transplantation of bone marrow cells from Berkeley SCD mice into lethally irradiated 6–8-wk-old C57BL/6 mice as previously described (Hidalgo et al., 2009; Turhan et al., 2002; Zhang et al., 2015). These BMT SCD mice were analyzed for reconstitution efficiency ≥ 3 mo after transplantation. Fully reconstituted mice (>97%) were used for experiments and are referred to here as SCD mice; Berkeley SCD mice are referred to as genetic SCD mice.

Flow cytometry

Cells were surface stained in PEB buffer (PBS supplemented with 0.5% BSA and 2 mM EDTA) for 30 min at 4°C in the dark. Multiparametric flow cytometric analyses were performed on a LSRII equipped with FACS Diva 6.1 software (BD Biosciences) and analyzed with FlowJo software (TreeStar). Dead cells were excluded by forward and side scatter and DAPI (Sigma-Aldrich) staining. Neutrophils were gated by Gr-1^{hi} CD115^{lo} SSC^{hi}. Aged neutrophils were gated by CD62L^{low} CXCR4^{high} within the neutrophil gate. Fluorophore-conjugated antibodies against mouse Gr-1 (RB6-8C5), CD115 (AFS98), and CXCR4 (2B11) were

purchased from eBioscience. Antibody specific to CD62L (MEL-14) was purchased from BD Biosciences.

Hematologic parameters

Blood was collected in 0.5 M EDTA, pH 8.0, through the retro-orbital sinus. WBC count, RBC count, and hemoglobin concentration were determined using an ADVIA 120 Hematology System (Siemens).

Intravital microscopy analysis of VOE

Experimental procedures and data analyses were performed as previously described (Turhan et al., 2002; Zhang et al., 2015). Briefly, male SCD mice were treated i.p. with 0.5 μ g TNF α (R&D Systems) and anesthetized 2 h later with an i.p. injection of a mixture of 2% chloralose (Sigma-Aldrich) and 10% urethane (Sigma-Aldrich) in PBS. Tracheal intubation was performed to ensure normal respiration after anesthesia. The cremaster muscle was gently exteriorized, mounted onto a microscopic stage, and superfused with Ringer's solution (pH 7.4, 37°C) aerated with a mixture of 95% N₂ and 5% CO₂. Postcapillary venules (18–25- μ m diameter) were recorded using a custom-designed upright microscope equipped with a 60 \times water-immersion objective and a charge-coupled device video camera (Hamamatsu). The adhesion fraction was quantified as the number of leukocytes remaining stationary for >20 s within a 100- μ m venular segment. In this model, >90% of adherent leukocytes are neutrophils, based on previous studies (Chiang et al., 2007). WBC–RBC interactions were defined as the associations between an RBC and an adherent leukocyte for ≥ 1 s and quantified as the number of interactions within a 100- μ m vessel segment/min per adherent leukocyte. Rolling cells along venules within 1 min were quantified. Venular diameters were measured using a video caliper, and centerline red cell velocity (V_{RBC}) for each recorded venule was measured using an optical Doppler velocimeter (Texas A&M). Blood flow rate (Q) was calculated as $Q = V_{mean} \times \pi d^2/4$, where d is venule diameter, and centerline velocity (V_{mean}) is estimated as $V_{RBC}/1.6$. Survival times, defined as the time from TNF α injection until death, were recorded.

Biomarker analysis

Plasma levels of ALT and AST were measured on a Beckman Coulter AU480 Chemistry Analyzer in the Biomarker Analytic Research Core at Albert Einstein College of Medicine.

Histopathology

Organs were excised and fixed in 10% neutral buffered formalin for 48–72 h and routinely processed for paraffin embedding. Samples for histopathology diagnostics were sectioned to a thickness of 5 μ m and stained with H&E. Images were taken using a P250 slide scanner in the Analytical Imaging Facility at Albert Einstein College of Medicine.

Measurement of urine osmolality

Mice were deprived of water for 16 h before urine collection. Urine osmolality was measured with a Model 3320 Osmometer according to the manufacturer's protocol (Advanced Instrument).

Microosmotic pump implantation

100 μ l of PBS or CGRP solution (0.3125 mg/ml; Tocris Bioscience) was injected into the ALZET microosmotic pumps (model 1007D). The micropumps were left in PBS at 37°C overnight for equilibration and then implanted subcutaneously into the SCD mice.

Capsaicin diet

The customized capsaicin-containing diet (100 ppm; capsaicin purchased from Sigma-Aldrich) and standard diets were generated by Tekland Diets at Evigo.

Forskolin treatment

Forskolin (Cayman Chemical) was given i.p. at 2 mg/kg twice a day for 5 d, and control mice were treated with vehicle control (DMSO) in PBS.

Behavioral testing

Thermal nociceptive responses were determined by measuring the latency to paw withdrawal using the Hargreaves apparatus (IITC Plantar Analgesia Meter; IITC Life Science). This assay was done blinded to different treatments. Briefly, male SCD mice were placed in a clear plastic cage and allowed to acclimatize for 1 h. The glass base temperature was 30°C (\pm 1°C). The aiming light (no thermal stimulus) was used to direct the source to the plantar surface of the paw. Stimuli of a given intensity, designated active intensity as percentage of maximum intensity of the apparatus, were presented until there were three or four unequivocal withdrawal responses to the stimulus. A withdrawal response was defined as a rapid, reflexive lifting or moving of the stimulated paw. Voluntary movement or ambiguous responses were not recorded. Stimuli were presented to alternating hind paws, with 5–10 min between stimulus presentations. The mean latency to withdraw the paw is presented and analyzed. This test was performed at the Rodent Behavior Core at Albert Einstein College of Medicine.

Quantification and statistical analyses

Results are presented as means \pm SEM. Statistical analyses were performed with Prism 7 and 8 (GraphPad Software). Unpaired two-sided Student's *t* tests (two-tailed) were used to compare two groups. One-way ANOVA was used for multiple group comparisons using Tukey's multiple comparisons test provided in Prism. Mantel-Cox test (log-rank test) was used to compare survival curves.

Online supplemental material

Fig. S1 provides additional information for Figs. 1 and 2 and shows the degree of anemia in SCD mice with depletion of nociceptors or CGRP administration. Fig. S2 relates to Fig. 2 and shows the effect of forskolin on VOE. Fig. S3 relates to Figs. 3 and 4 and shows the water/food consumption, body weight, and degree of anemia in SCD mice after short-term or long-term capsaicin-diet or standard-diet treatment, and the nociception of SCD mice after capsaicin-diet or standard-diet treatment. Table S1, Table S2, Table S3, Table S4, and Table S5 provide additional hemodynamic parameter data for Figs. 1–3 and Fig.

S2. Video 1 and Video 2 relate to Fig. 4 and show the behavior of SCD mice treated with the standard diet and capsaicin diet, respectively.

Acknowledgments

We thank Colette Prophete, George Amatuni, Xizhe Wang, and Peng Guo for technical assistance and members of the Frenette laboratory for helpful discussions, in particular Dr. Xin Gao for helpful advice. We thank Dr. Kathleen M. Caron (University of North Carolina, Chapel Hill, NC) for providing *Ramp1*^{−/−} mice.

This work was supported by National Institutes of Health RO grants (HL069438, DK056638, DK116312, and DK112976 to P.S. Frenette). The Biomarker Analytic Research Core is supported by an Institute for Clinical and Translational Research Einstein-Montefiore Clinical and Translational Science Award grant (5UL1TR002556) and an Einstein-Mount Sinai Diabetes Research Center grant (P30-DK020541). The Analytical Imaging Facility was supported by a National Institutes of Health Shared Instrumentation Grant (1S10OD019961). The Rodent Behavior Core was supported by a Rose F. Kennedy Intellectual and Developmental Disabilities Research Center grant (P30 HD071593).

Author contributions: C. Xu conceived and designed the research, performed experiments, collected and analyzed data, and wrote the manuscript. M. Gulinello performed the Hargreaves test. P.S. Frenette designed and supervised the research and wrote the manuscript.

Disclosures: P.S. Frenette reported grants from the National Institutes of Health during the conduct of the study; personal fees from Pfizer, grants from Ironwood Pharmaceuticals, and "other" from Cygnal Therapeutics outside the submitted work. He has served as consultant for Pfizer, received research funding from Ironwood Pharmaceuticals, and owns shares of Cygnal Therapeutics. No other disclosures were reported.

Submitted: 13 January 2020

Revised: 17 June 2020

Accepted: 27 August 2020

References

- Aich, A., M.K. Jones, and K. Gupta. 2019. Pain and sickle cell disease. *Curr. Opin. Hematol.* 26:131–138. <https://doi.org/10.1097/MOH.0000000000000491>
- Ballas, S.K., K. Gupta, and P. Adams-Graves. 2012. Sickle cell pain: a critical reappraisal. *Blood.* 120:3647–3656. <https://doi.org/10.1182/blood-2012-04-383430>
- Baral, P., B.D. Umans, L. Li, A. Wallrapp, M. Bist, T. Kirschbaum, Y. Wei, Y. Zhou, V.K. Kuchroo, P.R. Burkett, et al. 2018. Nociceptor sensory neurons suppress neutrophil and $\gamma\delta$ T cell responses in bacterial lung infections and lethal pneumonia. *Nat. Med.* 24:417–426. <https://doi.org/10.1038/nm.4501>
- Basbaum, A.I., D.M. Bautista, G. Scherrer, and D. Julius. 2009. Cellular and molecular mechanisms of pain. *Cell.* 139:267–284. <https://doi.org/10.1016/j.cell.2009.09.028>
- Carroll, C.P., S. Lanzkron, C. Haywood, Jr., K. Kiley, M. Pejsa, G. Moscou-Jackson, J.A. Haythornthwaite, and C.M. Campbell. 2016. Chronic Opioid Therapy and Central Sensitization in Sickle Cell Disease. *Am. J. Prev. Med.* 51(1, Suppl 1):S69–S77. <https://doi.org/10.1016/j.amepre.2016.02.012>
- Casanova-Acebes, M., C. Pitaval, L.A. Weiss, C. Nombela-Arrieta, R. Chèvre, N. A-González, Y. Kunisaki, D. Zhang, N. van Rooijen, L.E. Silberstein,

- et al. 2013. Rhythmic modulation of the hematopoietic niche through neutrophil clearance. *Cell*. 153:1025–1035. <https://doi.org/10.1016/j.cell.2013.04.040>
- Caterina, M.J., M.A. Schumacher, M. Tominaga, T.A. Rosen, J.D. Levine, and D. Julius. 1997. The capsaicin receptor: a heat-activated ion channel in the pain pathway. *Nature*. 389:816–824. <https://doi.org/10.1038/39807>
- Chen, G., J. Chang, D. Zhang, S. Pinho, J.E. Jang, and P.S. Frenette. 2016. Targeting Mac-1-mediated leukocyte-RBC interactions uncouples the benefits for acute vaso-occlusion and chronic organ damage. *Exp. Hematol.* 44:940–946. <https://doi.org/10.1016/j.exphem.2016.06.252>
- Chiang, E.Y., A. Hidalgo, J. Chang, and P.S. Frenette. 2007. Imaging receptor microdomains on leukocyte subsets in live mice. *Nat. Methods*. 4: 219–222. <https://doi.org/10.1038/nmeth1018>
- Chiu, I.M., B.A. Heesters, N. Ghasemlou, C.A. Von Hehn, F. Zhao, J. Tran, B. Wainger, A. Strominger, S. Muralidharan, A.R. Horswill, et al. 2013. Bacteria activate sensory neurons that modulate pain and inflammation. *Nature*. 501:52–57. <https://doi.org/10.1038/nature12479>
- Cohen, J.A., T.N. Edwards, A.W. Liu, T. Hirai, M.R. Jones, J. Wu, Y. Li, S. Zhang, J. Ho, B.M. Davis, et al. 2019. Cutaneous TRPV1⁺ Neurons Trigger Protective Innate Type 17 Anticipatory Immunity. *Cell*. 178:919–932.e14.
- Derry, S., R. Lloyd, R.A. Moore, and H.J. McQuay. 2009. Topical capsaicin for chronic neuropathic pain in adults. *Cochrane Database Syst. Rev.* (4). CD007393.
- Godinho-Silva, C., F. Cardoso, and H. Veiga-Fernandes. 2019. Neuro-Immune Cell Units: A New Paradigm in Physiology. *Annu. Rev. Immunol.* 37: 19–46. <https://doi.org/10.1146/annurev-immunol-042718-041812>
- Hargreaves, K., R. Dubner, F. Brown, C. Flores, and J. Joris. 1988. A new and sensitive method for measuring thermal nociception in cutaneous hyperalgesia. *Pain*. 32:77–88. [https://doi.org/10.1016/0304-3959\(88\)90026-7](https://doi.org/10.1016/0304-3959(88)90026-7)
- Hidalgo, A., J. Chang, J.E. Jang, A.J. Peired, E.Y. Chiang, and P.S. Frenette. 2009. Heterotypic interactions enabled by polarized neutrophil microdomains mediate thromboinflammatory injury. *Nat. Med.* 15: 384–391. <https://doi.org/10.1038/nm.1939>
- Hillery, C.A., P.C. Kerstein, D. Vilceanu, M.E. Barabas, D. Retherford, A.M. Brandow, N.J. Wandersee, and C.L. Stucky. 2011. Transient receptor potential vanilloid 1 mediates pain in mice with severe sickle cell disease. *Blood*. 118:3376–3383. <https://doi.org/10.1182/blood-2010-12-327429>
- Khasabova, I.A., M. Uhelski, S.G. Khasabov, K. Gupta, V.S. Seybold, and D.A. Simone. 2019. Sensitization of nociceptors by prostaglandin E₂-glycerol contributes to hyperalgesia in mice with sickle cell disease. *Blood*. 133: 1989–1998. <https://doi.org/10.1182/blood-2018-11-884346>
- Li, M., S.E. Wetzel-Strong, X. Hua, S.L. Tilley, E. Oswald, M.F. Krummel, and K.M. Caron. 2014. Deficiency of RAMP1 attenuates antigen-induced airway hyperresponsiveness in mice. *PLoS One*. 9. e102356. <https://doi.org/10.1371/journal.pone.0102356>
- McLatchie, L.M., N.J. Fraser, M.J. Main, A. Wise, J. Brown, N. Thompson, R. Solari, M.G. Lee, and S.M. Foord. 1998. RAMPs regulate the transport and ligand specificity of the calcitonin-receptor-like receptor. *Nature*. 393:333–339. <https://doi.org/10.1038/30666>
- Nagashima, H., T. Mahlaköiv, H.Y. Shih, F.P. Davis, F. Meylan, Y. Huang, O.J. Harrison, C. Yao, Y. Mikami, J.F. Urban, Jr., et al. 2019. Neuropeptide CGRP Limits Group 2 Innate Lymphoid Cell Responses and Constrains Type 2 Inflammation. *Immunity*. 51:682–695.e6.
- Nasimuzzaman, M., P.I. Arumugam, E.S. Mullins, J.M. James, K. Vanden-Heuvel, M.G. Narciso, M.A. Shaw, S. McGraw, B.J. Aronow, and P. Malik. 2019. Elimination of the fibrinogen integrin $\alpha_{M}\beta_{2}$ -binding motif improves renal pathology in mice with sickle cell anemia. *Blood Adv.* 3: 1519–1532. <https://doi.org/10.1182/bloodadvances.2019032342>
- Nath, K.A., and R.P. Hebbel. 2015. Sickle cell disease: renal manifestations and mechanisms. *Nat. Rev. Nephrol.* 11:161–171. <https://doi.org/10.1038/nrneph.2015.8>
- Oetjen, L.K., M.R. Mack, J. Feng, T.M. Whelan, H. Niu, C.J. Guo, S. Chen, A.M. Trier, A.Z. Xu, S.V. Tripathi, et al. 2017. Sensory Neurons Co-opt Classical Immune Signaling Pathways to Mediate Chronic Itch. *Cell*. 171:217–228.e13.
- Piel, F.B., M.H. Steinberg, and D.C. Rees. 2017. Sickle Cell Disease. *N. Engl. J. Med.* 376:1561–1573. <https://doi.org/10.1056/NEJMra1510865>
- Pinho-Ribeiro, F.A., B. Baddal, R. Haarsma, M. O'Seaghdha, N.J. Yang, K.J. Blake, M. Portley, W.A. Verri, J.B. Dale, M.R. Wessels, et al. 2018. Blocking Neuronal Signaling to Immune Cells Treats Streptococcal Invasive Infection. *Cell*. 173:1083–1097.e22.
- Riol-Blanco, L., J. Ordoñas-Montanes, M. Perro, E. Naval, A. Thiriot, D. Alvarez, S. Paust, J.N. Wood, and U.H. von Andrian. 2014. Calcitonin sensory neurons drive interleukin-23-mediated psoriasisform skin inflammation. *Nature*. 510:157–161. <https://doi.org/10.1038/nature13199>
- Russell, F.A., R. King, S.J. Smillie, X. Kodji, and S.D. Brain. 2014. Calcitonin gene-related peptide: physiology and pathophysiology. *Physiol. Rev.* 94: 1099–1142. <https://doi.org/10.1152/physrev.00034.2013>
- Sadler, K.E., K.J. Zappia, C.L. O'Hara, S.N. Langer, A.D. Weyer, C.A. Hillery, and C.L. Stucky. 2018. Chemokine (c-c motif) receptor 2 mediates mechanical and cold hypersensitivity in sickle cell disease mice. *Pain*. 159:1652–1663. <https://doi.org/10.1097/j.pain.0000000000001253>
- Sundd, P., M.T. Gladwin, and E.M. Novelli. 2019. Pathophysiology of Sickle Cell Disease. *Annu. Rev. Pathol.* 14:263–292. <https://doi.org/10.1146/annurev-pathmechdis-012418-012838>
- Talbot, S., R.E. Abdunour, P.R. Burkett, S. Lee, S.J. Cronin, M.A. Pascal, C. Laedermann, S.L. Foster, J.V. Tran, N. Lai, et al. 2015. Silencing Nociceptor Neurons Reduces Allergic Airway Inflammation. *Neuron*. 87: 341–354. <https://doi.org/10.1016/j.neuron.2015.06.007>
- Turhan, A., L.A. Weiss, N. Mohandas, B.S. Collier, and P.S. Frenette. 2002. Primary role for adherent leukocytes in sickle cell vascular occlusion: a new paradigm. *Proc. Natl. Acad. Sci. USA*. 99:3047–3051. <https://doi.org/10.1073/pnas.052522799>
- Van Eeden, S.F., S. Bicknell, B.A. Walker, and J.C. Hogg. 1997. Polymorphonuclear leukocytes L-selectin expression decreases as they age in circulation. *Am. J. Physiol.* 272:H401–H408.
- Vincent, L., D. Vang, J. Nguyen, M. Gupta, K. Luk, M.E. Ericson, D.A. Simone, and K. Gupta. 2013. Mast cell activation contributes to sickle cell pathobiology and pain in mice. *Blood*. 122:1853–1862. <https://doi.org/10.1182/blood-2013-04-498105>
- Wallrapp, A., P.R. Burkett, S.J. Riesenfeld, S.J. Kim, E. Christian, R.E. Abdunour, P.I. Thakore, A. Schnell, C. Lambden, R.H. Herbst, et al. 2019. Calcitonin Gene-Related Peptide Negatively Regulates Alarmin-Driven Type 2 Innate Lymphoid Cell Responses. *Immunity*. 51:709–723.e6.
- Ware, R.E., M. de Montalembert, L. Tshilolo, and M.R. Abboud. 2017. Sickle cell disease. *Lancet*. 390:311–323. [https://doi.org/10.1016/S0140-6736\(17\)30193-9](https://doi.org/10.1016/S0140-6736(17)30193-9)
- Zhang, D., G. Chen, D. Manwani, A. Mortha, C. Xu, J.J. Faith, R.D. Burk, Y. Kunisaki, J.-E. Jang, C. Scheiermann, et al. 2015. Neutrophil ageing is regulated by the microbiome. *Nature*. 525:528–532. <https://doi.org/10.1038/nature15367>
- Zhang, D., C. Xu, D. Manwani, and P.S. Frenette. 2016. Neutrophils, platelets, and inflammatory pathways at the nexus of sickle cell disease pathophysiology. *Blood*. 127:801–809. <https://doi.org/10.1182/blood-2015-09-618538>

Supplemental material

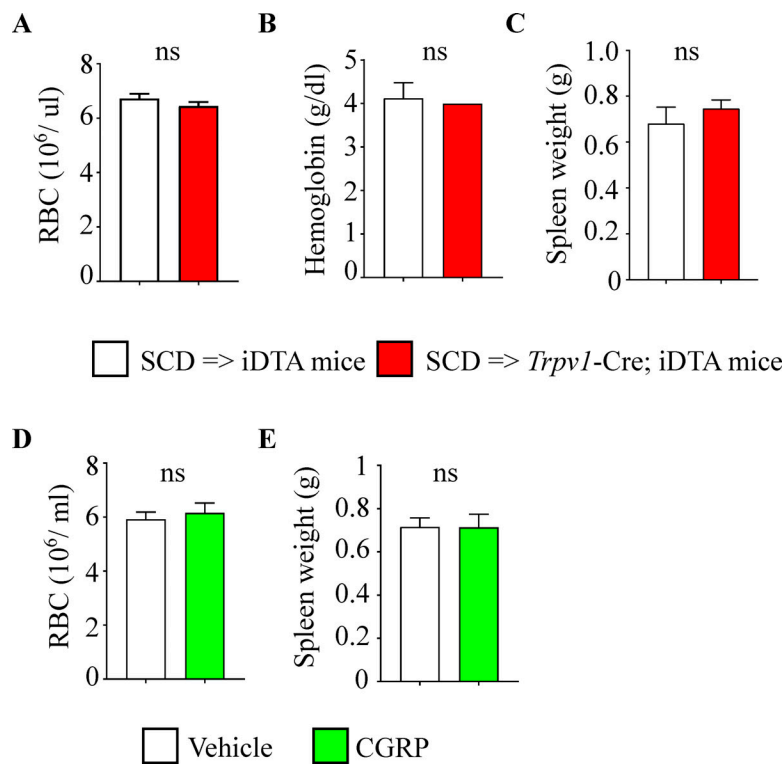


Figure S1. **Depletion of nociceptors and CGRP administration have no effect on the degree of anemia in SCD mice.** (A) Number of RBCs in the peripheral blood of SCD \rightarrow iDTA mice ($n = 8$) and SCD \rightarrow *Trpv1*-Cre; iDTA mice ($n = 4$). (B) Plasma hemoglobin concentrations of SCD \rightarrow iDTA mice ($n = 8$) and SCD \rightarrow *Trpv1*-Cre; iDTA mice ($n = 4$). (C) Spleen weights of SCD \rightarrow iDTA mice ($n = 8$) and SCD \rightarrow *Trpv1*-Cre; iDTA mice ($n = 4$). (D) Number of RBCs in vehicle-treated SCD mice ($n = 5$) and CGRP-treated SCD mice ($n = 5$). (E) Spleen weights of vehicle-treated SCD mice ($n = 5$) and CGRP-treated SCD mice ($n = 5$). Error bars, mean \pm SEM. Data represent at least two independent experiments analyzed using unpaired Student's t test. ns, not significant.

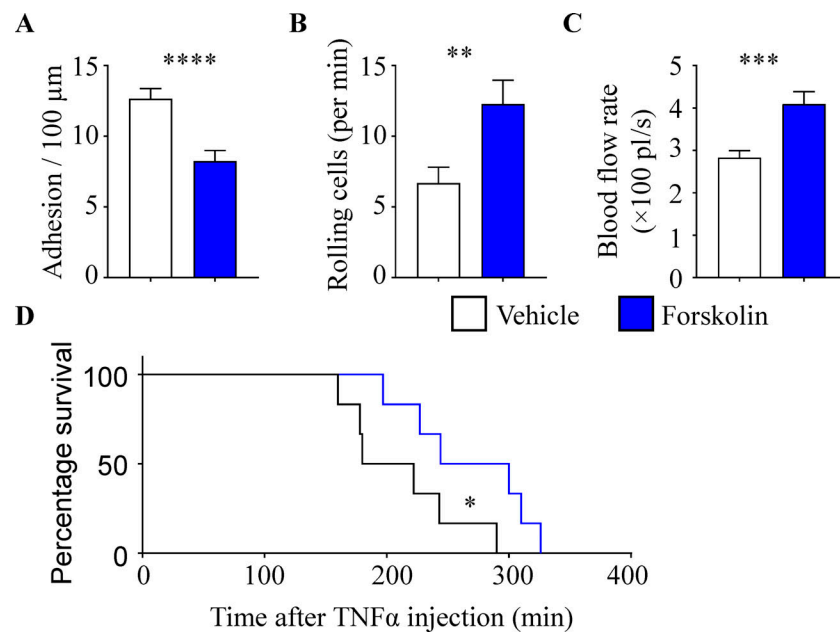


Figure S2. **Forskolin protects SCD mice from VOE.** SCD mice were treated with forskolin for 5 d and challenged in the TNF α /surgical trauma-induced VOE model. **(A–C)** Number of adherent leukocytes (A), number of rolling leukocytes (B), and blood flow rate (C) in the postcapillary collecting venules of cremaster muscle in vehicle-treated SCD mice ($n = 32$ venules from six mice) and forskolin-treated SCD mice ($n = 29$ venules from six mice) analyzed by intravital microscopy. **(D)** Survival time of vehicle-treated SCD mice ($n = 6$) and forskolin-treated SCD mice ($n = 6$) in TNF α -induced acute vaso-occlusion. Error bars, mean \pm SEM; *, $P < 0.05$; **, $P < 0.01$; ***, $P < 0.001$; ****, $P < 0.0001$. Data analyzed using unpaired Student's t test in A–C and Mantel–Cox test (log-rank) for the survival analysis in D.

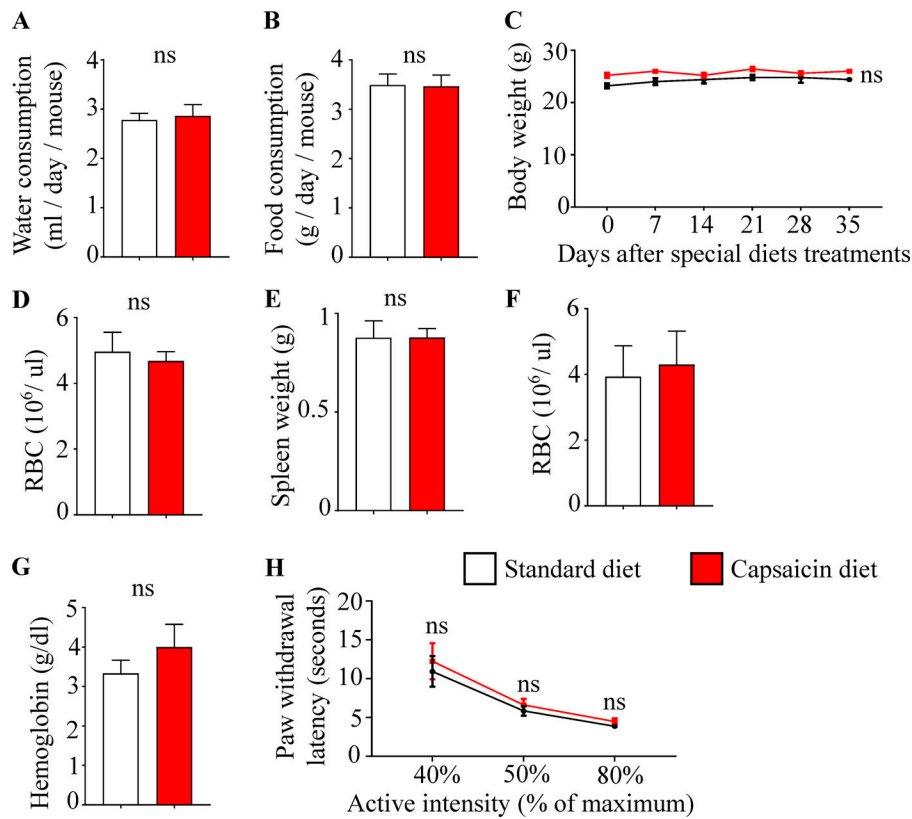


Figure S3. Capsaicin diet treatment did not change water/food consumption, body weight, or the degree of anemia in SCD mice. (A and B) Water consumption (A) and food consumption (B) of SCD mice fed with standard chow ($n = 10$) and capsaicin-containing diet ($n = 10$). **(C)** Body weight of SCD mice fed with standard chow ($n = 5$) and capsaicin-containing diet ($n = 5$). **(D)** Number of RBCs in the SCD mice fed with standard chow ($n = 5$) and capsaicin-containing diet ($n = 5$) for 6 wk. **(E)** Spleen weights of SCD mice fed with standard chow ($n = 5$) and capsaicin-containing diet ($n = 5$) for 6 wk. **(F)** Number of RBCs in standard diet-treated SCD mice ($n = 5$) and capsaicin diet-treated SCD mice ($n = 5$) 14 mo after treatment. **(G)** Plasma hemoglobin concentrations of standard diet-treated SCD mice ($n = 5$) and capsaicin diet-treated SCD mice ($n = 5$) 14 mo after treatment. **(H)** Paw withdrawal latency. SCD mice were fed with standard chow ($n = 10$) and capsaicin-containing diet ($n = 8$) for 2 mo, and heat sensitivity was determined using the Hargreaves test. Active intensity means the percentage of the maximum intensity of the Hargreaves apparatus. Error bars, mean \pm SEM. ns, not significant.

Video 1. **SCD mice on control diet.** SCD mice were treated with control diet. The video was recorded 14 mo after the initiation of treatment.

Video 2. **SCD mice on capsaicin diet.** SCD mice were treated with capsaicin diet. The video was recorded 14 mo after the initiation of treatment.

Tables S1–S5 are provided online. Table S1 shows hemodynamic parameters in SCD \rightarrow iDTA mice and SCD \rightarrow *Trpv1-Cre*; iDTA mice. Table S2 shows hemodynamic parameters in vehicle-treated SCD mice and CGRP-treated SCD mice. Table S3 shows hemodynamic parameters in vehicle-treated SCD mice and forskolin-treated SCD mice. Table S4 shows hemodynamic parameters in SCD \rightarrow *Ramp1*^{+/+} mice and SCD \rightarrow *Ramp1*^{-/-} mice. Table S5 shows hemodynamic parameters in SCD mice fed with a standard diet and the capsaicin diet.